

## Universal Profile of the Vortex Condensate in Two-Dimensional Turbulence

Jason Laurie,<sup>1,\*</sup> Guido Boffetta,<sup>2</sup> Gregory Falkovich,<sup>1,3</sup> Igor Kolokolov,<sup>4,5</sup> and Vladimir Lebedev<sup>4,5</sup>

<sup>1</sup>*Physics of Complex Systems, Weizmann Institute of Science, Rehovot 76100, Israel*

<sup>2</sup>*Dipartimento di Fisica and INFN, Università di Torino, via P. Giuria 1, 10125 Torino, Italy*

<sup>3</sup>*Institute for Information Transmission Problems, Moscow 127994, Russia*

<sup>4</sup>*Landau Institute for Theoretical Physics, Kosygina 2, Moscow 119334, Russia*

<sup>5</sup>*Moscow Institute of Physics and Technology, Dolgoprudny, Moscow 141700, Russia*

(Received 5 June 2014; published 17 December 2014)

An inverse turbulent cascade in a restricted two-dimensional periodic domain creates a condensate—a pair of coherent system-size vortices. We perform extensive numerical simulations of this system and carry out theoretical analysis based on momentum and energy exchanges between the turbulence and the vortices. We show that the vortices have a universal internal structure independent of the type of small-scale dissipation, small-scale forcing, and boundary conditions. The theory predicts not only the vortex inner region profile, but also the amplitude, which both perfectly agree with the numerical data.

DOI: [10.1103/PhysRevLett.113.254503](https://doi.org/10.1103/PhysRevLett.113.254503)

PACS numbers: 47.27.Gs, 47.10.-g

From both a fundamental and practical perspective, a central problem of turbulence theory is in the understanding and the description of the interaction of turbulence fluctuations with a mean (coherent) flow [1]. Even at the most basic level of energy and momentum budget, such an interaction is quite nontrivial: we expect energy to go from the flow to turbulence in the fully three-dimensional case, while it can go from turbulence to the flow in two dimensions (2D) [2] or in thin fluid layers [3]. At present, there is no unified conceptual framework to address this problem. The cases most studied (for over a century) are flows in channels or pipes. Despite this, even basic problems, like determining at which mean velocity turbulent fluctuations are sustained, are still objects of intense investigations [4], nor is there any consistent theory for the mean profile so that even the celebrated logarithmic law is a subject of controversy [5]. Here, we consider 2D turbulence where small-scale fluctuations excited by pumping transfer energy to larger scales by an inverse cascade [2,3,6].

Already, the first experiments on 2D turbulence in thin layers [7] have shown that in a finite system with weak bottom friction, the inverse cascade leads to the formation of coherent vortices. Subsequent direct numerical simulations [8] and experiments [9] demonstrated that these vortices have well-defined and reproducible mean profiles with a radial power-law decay of vorticity in the inner region. Moreover, the profile in that region depends neither on the boundary conditions (periodic in numerics, no-slip in experiments) nor on the type of forcing (random in numerics versus parametric excitation or electromagnetic force in experiments). Even more remarkable, the profile is similar when modeling without linear (bottom) friction at intermediate times where the vortices slowly grow [8] until eventually viscosity stabilizes the system [10]. Here we present the results of new extensive simulations of 2D

turbulence in a periodic box. By including linear friction, we are able to reach a statistically steady state and collect considerable statistics. Our results show that the internal structure does not depend on the type of (hyper)-viscosity nor on the value of the linear friction (as long as it is small enough for condensation). One can thus conclude that the profile in the inner region is universal since it depends on neither the excitation mechanism, boundary conditions, nor the dissipation mechanisms. This is also revealed by a new theoretical framework for the analysis of turbulence-flow interaction, which is developed below. The theory explains the numerical results and gives new insight into the coherent vortex formation and structure.

Both theory and numerics use the forced 2D Navier-Stokes equation for the 2D velocity  $\mathbf{v}$  with linear friction,

$$\partial_t \mathbf{v} + \alpha \mathbf{v} + (\mathbf{v} \cdot \nabla) \mathbf{v} = -\nabla p + \nu \Delta \mathbf{v} + \mathbf{f}, \quad (1)$$

where  $\nu$  is the kinematic viscosity. The external random force (per unit mass),  $\mathbf{f}$ , has homogeneous statistics, with the correlation time small enough and the correlation length much less than the system size  $L$ . The friction coefficient  $\alpha$  is small compared to the inverse turnover time of the system-size vortices,  $\alpha^3 \ll \epsilon/L^2$ , where  $\epsilon = \langle \mathbf{f} \cdot \mathbf{v} \rangle$  is the energy production rate (per unit mass). The angular brackets designate temporal averaging.

In our simulations, we used a periodic square box of size  $L = 2\pi$  so that the Fourier grid spacing is  $dk = 2\pi/L = 1$ . We numerically solve (1) using a pseudospectral spatial method, fully dealiased by the two-thirds rule and time stepped by a second-order Runge-Kutta scheme. We initially perform three simulations at a spatial resolution of  $512 \times 512$ . The external forcing acts in Fourier space in an annulus of width  $3dk = 3$  centered around the forcing wave number  $k_f = 100$  with a constant amplitude of 0.1. We made several runs with small-scale (hyper)-viscous

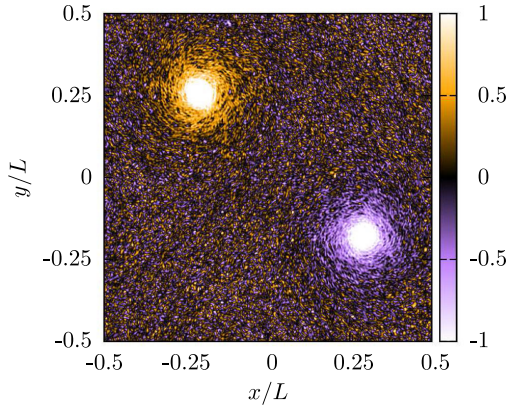


FIG. 1 (color online). Plot of the total vorticity normalized by  $(\epsilon/\alpha L^2)^{1/2}$  during the condensate regime of simulation B.

dissipation of the form  $\nu(-\Delta)^{2p}\nu$  for  $p = 1, 2, 3, 4$ , with all the results being quantitatively similar. We perform an additional simulation at resolution  $1024 \times 1024$  with a smaller scale forcing situated at  $k_f = 200$  with amplitude 0.16 to give a comparable  $\epsilon$ . The data presented are for the highest power of hyperviscosity considered:  $\nu(-\Delta)^8\nu$  with  $\nu = 5 \times 10^{-35}$  for  $512 \times 512$  and  $\nu = 7 \times 10^{-39}$  for  $1024 \times 1024$ , which gives the most extended inertial range in Fourier space and the widest inner vortex region.

The first three sets of simulations are all for  $512 \times 512$  but with different friction:  $\alpha = 1.1 \times 10^{-4}$  (A),  $6.4 \times 10^{-5}$  (B), and  $3.2 \times 10^{-5}$  (C), which give  $\epsilon = 3.47 \times 10^{-4}$  (A),  $3.57 \times 10^{-4}$  (B), and  $3.47 \times 10^{-4}$  (C). To better resolve the inner vortex region, we perform an additional simulation (D) at a spatial resolution of  $1024 \times 1024$  with  $\alpha = 6.7 \times 10^{-5}$ , resulting in  $\epsilon = 3.77 \times 10^{-4}$ . Each simulation is run until the system reaches a nonequilibrium stationary state through the balance of forcing and friction, observed by the saturation of the total kinetic energy  $E = (1/2) \int v^2 dx dy$ . Once stationary, we output data at every large eddy turnover time (estimated by assuming that the total energy is dominated by the condensate at the largest scale) for  $4 \times 10^4$  turnover times. Because of the increased resolution and the subsequent additional computation expense, simulation D was only performed for  $2 \times 10^2$  turnover times. A typical snapshot of the vorticity field in the stationary state is plotted in Fig. 1. For disentangling the mean flow from the turbulence, it is crucial to locate the vortex center and then to follow it as the vortex pair wanders in space. For each time frame, we locate the center of the (positive) vortex by determining the global maximum of the vorticity and then computing the center of mass of the vorticity in a box of  $8 \times 8$  grid points around the extremum. Subsequently, we shift the domain at every step so that the vortex center is at the origin.

The temporal average over all time frames of the centered vortex filters out the zero-mean fluctuations and gives the mean vorticity distribution. Subtracting the mean flow from the original vorticity gives the fluctuations. We double the statistics by applying the same method to

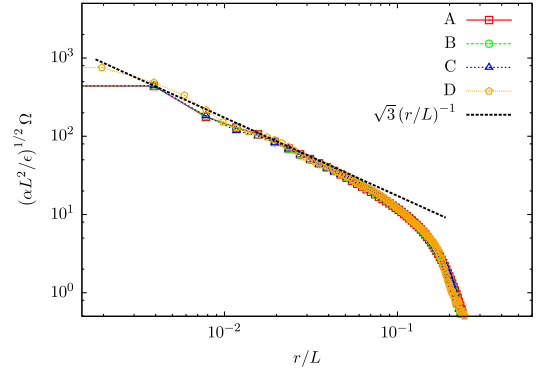


FIG. 2 (color online). Radial profile of the mean vorticity  $\Omega$  normalized by  $(\epsilon/\alpha L^2)^{1/2}$ . The straight black dashed line corresponds to the theoretically predicted radial profile  $\sqrt{3}(r/L)^{-1}$  determined from Eq. (8).

the other (negative vorticity) vortex after the required vorticity-velocity symmetry transformations that permit us to change the sign of the vorticity. Results of the temporal averaging for the simulations with different linear friction coefficients are presented in Figs. 2–7. The amplitude of the final condensate apparently scales as  $\alpha^{-1/2}$ .

The mean velocity profile inside the vortex is highly isotropic. The vortex interior can be separated into the narrow vortex core and the region outside the core where the mean profile reveals some universal scaling properties. We focus on this universal behavior.

Let us now provide some basic theoretical analysis. We introduce polar coordinates with the origin at the vortex center:  $r$  is the distance from the center, and  $\varphi$  is the polar angle. Based on numerical simulations and experiments, we assume that the inner region of the vortex is isotropic and can be described in terms of the mean polar velocity  $U$  depending on  $r$ . The average vorticity is then  $\Omega = U/r + \partial_r U$ . Taking the curl of (1), neglecting the viscous term (assumed to be small for scales larger than the pumping length) and decomposing the mean from fluctuations, one obtains

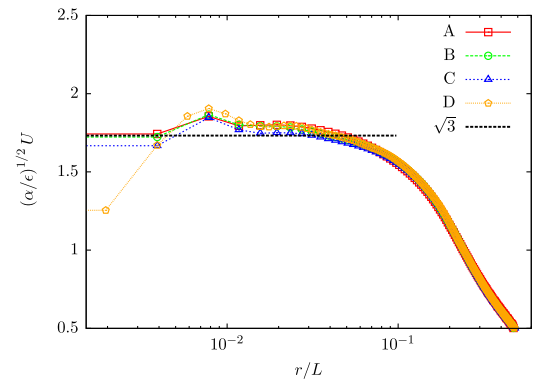


FIG. 3 (color online). Radial profile of the mean polar velocity  $U$  in log-lin coordinates. The horizontal black line is  $(\alpha/\epsilon)^{1/2}U = \sqrt{3}$  [Eq. (8)].

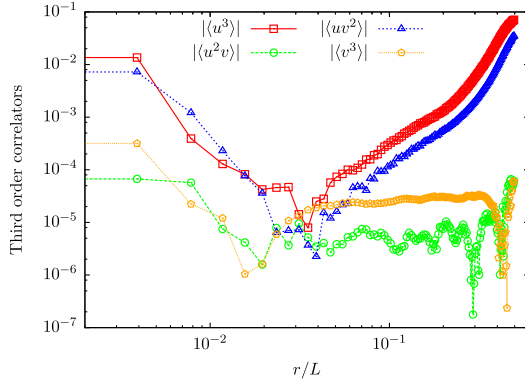


FIG. 4 (color online). Third-order moments,  $\langle u^3 \rangle$ ,  $\langle u^2 v \rangle$ ,  $\langle uv^2 \rangle$ , and  $\langle v^3 \rangle$  for simulation C: an additional smallness of all odd in  $v$  moments.

$$\alpha\Omega + \frac{1}{r}\partial_r(r\langle v\omega \rangle) = 0, \quad (2)$$

$$\begin{aligned} \partial_t\omega + \frac{U}{r}\partial_\varphi\omega + v\partial_r\omega + \alpha\omega \\ = -[v\partial_r + (u/r)\partial_\varphi]\omega - \alpha\Omega + \text{curl}f, \end{aligned} \quad (3)$$

where the radial velocity  $v$ , polar velocity  $u$ , and vorticity  $\omega$  describe the fluctuations.

An attempt to construct a theory explaining the power-law profile  $\Omega \propto r^{-a}$  was made in [11]. It was based on the existence of power-law zero modes of  $\omega$  on the background of the power-law mean vorticity  $\Omega$ . Assuming that the zero modes give the main contribution to the mean vorticity flux  $\langle v\omega \rangle$  and using perturbation theory (over nonlinear interaction), one relates  $a$  to the scaling of the hypothetical leading contribution to  $\langle v\omega \rangle$ . Equating scaling exponents of both parts of (2), one finds  $a = 5/4$  [11], which does not contradict the results of [8,9]. Our data, with higher resolution and increased statistics, suggest, however, that  $a \approx 1$  (see Fig. 2). This is even more clear from Fig. 3, which demonstrates that  $U$  is  $r$  independent inside the vortex, in accordance with  $\Omega \propto r^{-1}$ .

To explain the discrepancy between the zero-mode prediction and the actual profile, we note that the zero modes must give an anomalously small contribution to the average  $\langle v\omega \rangle$ . This follows from symmetry considerations applied to (3). If, as assumed in [11], the pumping term on the right-hand side can be neglected when the characteristic scale  $r$  exceeds the pumping correlation length, then by multiplying (3) by  $\omega^n$  and averaging over time one obtains

$$\langle v\omega^n \rangle \partial_r \Omega + \frac{\partial_r \langle rv\omega^{n+1} \rangle}{(n+1)r} + \alpha \langle \omega^{n+1} \rangle + \alpha \langle \omega^n \rangle \Omega = 0,$$

where we have used isotropy. From the relations for different  $n$ , it follows that the large-scale contributions to  $\langle v\omega^n \rangle$  are proportional to  $\alpha$ . Also all averages odd in  $v$  tend to zero as  $\alpha \rightarrow 0$ . On a deeper level, this follows from time

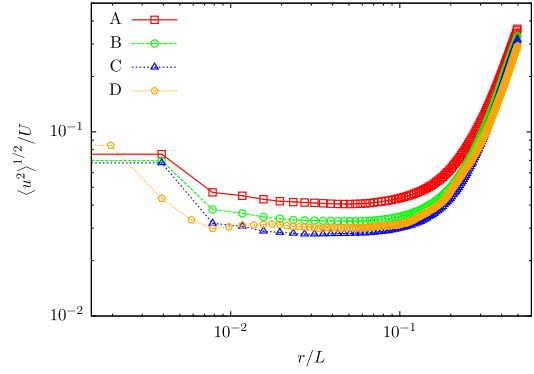


FIG. 5 (color online). Polar velocity fluctuations.

reversibility of the Euler equation, broken only by the linear friction term. The smallness of  $\langle v\omega^n \rangle$  for large-scale contributions implies the smallness of the respective correlation functions as well. This conclusion is supported by the data presented in Fig. 4.

Let us show now that the mean profile can be derived from the conservation laws. The Navier-Stokes equation (1) itself is the momentum conservation law. Taking the radial component and averaging it while exploiting isotropy and incompressibility,  $\partial_\varphi u + \partial_r(rv) = 0$ , one obtains

$$\partial_r \langle rv^2 \rangle + r\partial_r \langle p \rangle = U^2 + \langle u^2 \rangle. \quad (4)$$

The polar mean component of (1) is as follows:

$$r^{-1}\partial_r(r^2 \langle uv \rangle) = -\alpha r U. \quad (5)$$

The left-hand side of (5) is the divergence of the flux of the mean angular momentum  $rU$ , and so  $r\langle uv \rangle$  is the flux. When  $\langle uv \rangle$  is nonzero, the flow is irreversible; i.e. the sign of  $\langle uv \rangle$  does not change upon the transformation  $t \rightarrow -t$  while the sign of  $U$  does. If  $\langle uv \rangle$  does not decay faster than  $r^{-2}$ , then the signs of  $\langle uv \rangle$  and  $U$  are opposite, which implies that the momentum flows toward the vortex center (this is natural since the mean angular momentum density  $rU$  decreases towards the center).

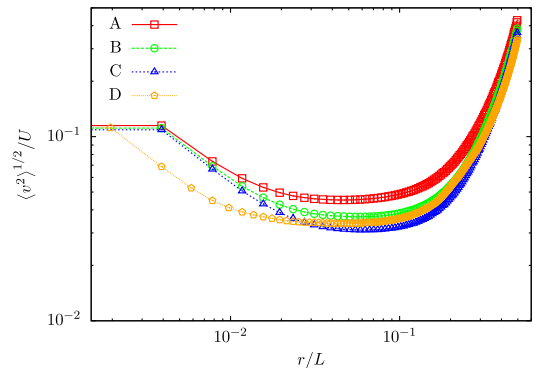


FIG. 6 (color online). Radial velocity fluctuations.

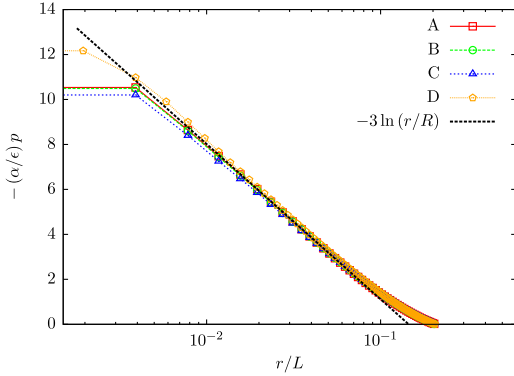


FIG. 7 (color online). Normalized radial pressure profile. The data are compared to the prediction (9) with  $R/L = 0.143$ .

Consider now the energy balance. By taking a scalar product of  $\mathbf{v}$  with (1) and averaging, one gets for the total energy density (containing both the mean flow and fluctuations):

$$\frac{1}{r} \partial_r \left[ rU \langle uv \rangle + r \left\langle v \left( \frac{u^2 + v^2}{2} + p \right) \right\rangle \right] + \alpha(U^2 + \langle u^2 + v^2 \rangle) = \langle \mathbf{f} \cdot \mathbf{v} \rangle. \quad (6)$$

In deriving (6), we have neglected, again, viscosity, which mainly influences the direct cascade, dissipating enstrophy (squared vorticity) but not energy [2] (in the numerics, we use hyperviscous dissipation).

We now consider the inner region of the vortex, where  $u, v \ll U$  (see Figs. 5 and 6), which demonstrate that fluctuations inside the vortex are suppressed compared with the mean flow. It is a consequence of the large mean velocity gradient  $\sim U/r$ , growing toward the center. The relative strength of the fluctuations increases as  $r$  grows, and on the periphery where  $r \simeq L$ , fluctuations become of the order of the mean flow. Considering the vortex interior, we neglect  $\langle u^2 + v^2 \rangle$  in comparison to  $U^2$ , and also odd in  $v$  terms since they contain two small parameters, related to the smallness of  $\alpha$  and that of the fluctuations. Substituting  $\langle \mathbf{f} \cdot \mathbf{v} \rangle = \epsilon$ , one obtains

$$\epsilon = \frac{1}{r} \partial_r (rU \langle uv \rangle) + \alpha U^2. \quad (7)$$

The same approximation is made in considering logarithmic turbulent boundary layers [12], but there  $\epsilon$  is the dissipation rate, whose coordinate dependence is unknown *a priori*. In our case,  $\epsilon$  is the pumping term independent of coordinates, which allows us to solve the problem. Combining (5) and (7) we find an  $r$ -independent mean polar velocity

$$U^2 = 3\epsilon/\alpha, \quad (8)$$

whose value and  $r$  independence are in excellent agreement with the numerics (see Figs. 2 and 3). Note that this vortex

profile is different from previously known cases (the Rankine vortex with uniform vorticity and the Lamb-Oseen vortex with a Gaussian distribution of vorticity) apparently due to the feeding by turbulence.

It follows from (8) that the second term in (7) is equal to  $2\epsilon$ ; i.e., at every point inside the vortex, the energy transfer from outside brings twice more than the local inverse cascade. Substituting (8) into (4) and neglecting  $u^2$  and  $v^2$  in comparison to  $U$ , we obtain for the pressure

$$p(r) = (3\epsilon/\alpha) \ln(r/R), \quad (9)$$

where  $R \sim L$ . We present the radial profile of the pressure around the vortex condensate in Fig. 7. One extracts from the numerical data  $R/L = 0.143$ , which is approximately the size of the vortex (see Fig. 2).

Let us stress that the analytical theory presented is explicitly universal. First, it does not depend on the boundary conditions. Second, only the mean energy flux  $\epsilon$ , which is an outcome of the interplay between the small-scale mechanisms of excitation and dissipation, enters into the theory, not the mechanisms themselves. This was confirmed in numerical simulations with different forms of forcing and dissipation. Third, it is straightforward to modify our theory for the frictionless case  $\alpha = 0$ . The time dependence of the mean velocity can be established from the fact that the total energy must grow as  $\epsilon t$  so that  $U(t) \propto \sqrt{t}$ , which was indeed observed in the numerics of Chertkov *et al.* [8] and also of Chan *et al.* [10] for intermediate times before viscosity stabilized the system. Subsequently, in all formulas (2)–(9), the time-derivative term replaces that of the linear friction with the substitution  $\alpha \rightarrow 1/t$ . The form of the mean profile remains the same, but, of course, all averages are now taken over a time interval  $\tau$  short compared with  $t$  but long compared with  $1/\Omega \simeq r/\sqrt{\epsilon t}$ , which requires  $t \gg r^{2/3} \epsilon^{-1/3}$ .

To conclude, we have developed a theory describing the mean velocity profile inside the coherent vortices. Within the vortex, we have found that velocity fluctuations are suppressed. Towards the periphery, velocity fluctuations become comparable to the mean flow, both of which can be estimated by  $(\epsilon/\alpha)^{1/2}$ , arising from the energy balance between production and friction. For small  $r$ , the constant  $U$  profile is correct down to the vortex core.

This work was supported by the HPC-EUROPA2 Project No. 228398 and the grants of the BSF and the Minerva Foundation. The analytical part of this work was also supported by the Russian Scientific Fund, Grant No. 14-22-00259.

\*Corresponding author.

jason.laurie@weizmann.ac.il

[1] A. A. Townsend, *The Structure of Turbulent Shear Flow* (Cambridge University Press, Cambridge, 1976).



- 
- [2] G. Boffetta and R. E. Ecke, *Annu. Rev. Fluid Mech.* **44**, 427 (2012).
- [3] H. Xia, D. Byrne, G. Falkovich, and M. Shats *Nat. Phys.* **7**, 321 (2011)
- [4] K. Avila, D. Moxey, A. de Lozar, M. Avila, D. Barkley, and B. Hof, *Science* **333**, 192 (2011).
- [5] M. Buschmann and M. Gad-el-Hak, *AIAA J.* **41**, 565 (2003).
- [6] R. H. Kraichnan, *Phys. Fluids* **10**, 1417 (1967).
- [7] J. Sommeria, *J. Fluid Mech.* **170**, 139 (1986).
- [8] M. Chertkov, C. Connaughton, I. Kolokolov, and V. Lebedev, *Phys. Rev. Lett.* **99**, 084501 (2007).
- [9] H. Xia, M. Shats, and G. Falkovich, *Phys. Fluids* **21**, 125101 (2009).
- [10] C.-K. Chan, D. Mitra, and A. Brandenburg, *Phys. Rev. E* **85**, 036315 (2012).
- [11] M. Chertkov, I. Kolokolov, and V. Lebedev, *Phys. Rev. E* **81**, 015302(R) (2010).
- [12] L. Landau and E. Lifshitz, *Fluid Mechanics* (Pergamon Press, Oxford, 1959).